• **Basic Research** •

A highly sensitive fluorescent probe RN-NA reveals peroxynitrite as a novel biomarker for primary open angle glaucoma

Bo Qin[1,2], Yuan Lei[1,2], Luo Bao[3], You–Jia Zhang[1,2], Ke–Yin Liu[3], Yu–Hong Chen[1,2]

[1]Department of Ophthalmology & Visual Science, Eye & ENT Hospital, Shanghai Medical College, Fudan University, Shanghai 200031, China

[2]Key Laboratory of Myopia, NHFPC (Fudan University), Shanghai Key Laboratory of Visual Impairment and Restoration (Fudan University), Shanghai 200031, China

[3]State Key Laboratory of Biobased Material and Green Papermaking, Key Laboratory of Pulp & Paper Science and Technology of Shandong Province/Ministry of Education, Qilu University of Technology, Shandong Academy of Sciences, Jinan 250353, Shandong Province, China

Co-first authors: Bo Qin and Yuan Lei

Correspondence to: Ke-Yin Liu. State Key Laboratory of Biobased Material and Green Papermaking, Key Laboratory of Pulp & Paper Science and Technology of Shandong Province/ Ministry of Education, Qilu University of Technology, Shandong Academy of Sciences, Jinan 250353, Shandong Province, China. keyinliu@163.com; Yu-Hong Chen. Key Laboratory of Myopia, NHFPC (Fudan University), Shanghai Key Laboratory of Visual Impairment and Restoration (Fudan University), Shanghai 200031, China. doctorrainbow@126.com

Abstract

● **AIM:** To directly quantify peroxynitrite ($ONOO^-$) using a highly sensitive fluorescence resonance energy transfer probe RN-NA, investigate the association between $ONOO^-$ and primary open angle glaucoma (POAG), and clarify whether RN-NA could be used as a potential tool for POAG diagnosis.

● **METHODS:** Plasma and aqueous humor (AH) samples were collected from POAG patients ($n=100$, age: 59.70±6.87y) and age-related cataract (ARC) patients ($n=100$, age: 61.15±4.60y) admitted to our hospital. Next, RN-NA was used to detect $ONOO^-$ in plasma and AH samples, and the relationship between $ONOO^-$ level and POAG was analyzed using binary logistic regression. Besides, Pearson correlation analysis was applied to characterize the correlation of the levels of $ONOO^-$ with the patients' age, intraocular pressure (IOP), and mean deviation of visual field testing. The $ONOO^-$ scavenger MnTMPyP was employed to treat the 3-morpholinosyndnomine (SIN-1)-induced ocular hypertension in mice ($n=7$, 6-8wk). Finally, the IOP and $ONOO^-$ in both eyes were measured 30min after the last drug treatment.

● **RESULTS:** $ONOO^-$ levels of AH and plasma were significantly higher in the POAG group than in the ARC group ($P<0.01$). Additionally, $ONOO^-$ levels were closely correlated with POAG in a binary logistic regression analysis [odds ratio (OR)=1.008, 95% confidence interval (CI): 1.002-1.013, $P<0.01$ for AH; OR=1.004, 95%CI: 1.002-1.006, $P<0.001$ for plasma]. Pearson correlation analysis showed that $ONOO^-$ levels in AH or plasma were positively associated with visual field defects ($R=0.51$, $P<0.01$ for AH; $R=0.45$, $P<0.001$ for plasma), and $ONOO^-$ levels in plasma and AH were correlated in the POAG group ($R=0.69$, $P<0.001$). However, administering MnTMPyP to mouse eyes reversed the elevated IOP caused by SIN-1 ($P<0.05$).

● **CONCLUSION:** $ONOO^-$ levels in AH and plasma, detected by RN-NA, are significantly related to POAG and positively correlated with visual field defects in POAG patients. Hence, $ONOO^-$ is a potential biomarker of POAG, especially advanced POAG. Besides, anti-nitration compounds may be novel ocular hypotensive agents based on the animal study.

● **KEYWORDS:** peroxynitrite; fluorescent probe RN-NA; primary open angle glaucoma; 3-morpholinosyndnomine

INTRODUCTION

Glaucoma, a neurodegenerative disease characterized by a progressive loss of retinal ganglion cells, is the main cause of irreversible vision impairment worldwide. Primary

open angle glaucoma (POAG) is one of the most common types of glaucoma, and elevated intraocular pressure (IOP) is its main risk factor[1]. Due to insidious nosogenesis and irreversible optic nerve damage, POAG patients with chronic progression has a poor visual prognosis. Therefore, both early diagnosis and prompt treatment of vision loss early are crucial to prevent irreversible damage in patients with POAG[2-3].

Nitrative stress plays a pathogenic role in POAG[4]. Peroxynitrite (ONOO$^-$) is a reactive nitrogen species (RNS) formed by the reaction between endogenous nitric oxide (NO) and free radical superoxide (O$_2^-$), which can modify essential cellular molecules such as proteins, DNA, and lipids[5]. 3-nitrotyrosine (3-NT) is the main chemical product and is used as a footprint of nitrative stress since it reflects the level of nitrative damage to proteins when detected with anti-nitrotyrosine antibodies[6-7]. Generally, the serum level of 3-NT in POAG patients is much higher than in controls, which suggests that elevated ONOO$^-$ can be a systemic risk factor for POAG[8]. But 3-NT does not represent the total concentration of ONOO$^-$, it only reflects the level of tyrosine nitration. Therefore, it is necessary to use a direct probe to accurately measure ONOO$^-$.

In previous research, we had constructed a fluorescent probe RN-NA for detection of ONOO$^-$ in our laboratory[9]. RN-NA is composed by two dyes, RN and NA, and fluorescence resonance energy transfer (FRET) process was formed between the two dyes. The probe exhibited good fluorescence response toward ONOO$^-$ in cells and zebrafish model constructed. In the presence of ONOO$^-$, the two dyes RN and NA can give obvious light changes in the green and red channels. Therefore, ONOO$^-$ induced fluorescence changes in the RN-NA probe, which provides a fast and stable method of detecting the level of ONOO$^-$ in the plasma or other body fluids.

The objective of this study was to measure the concentration of ONOO$^-$ in human samples using RN-NA to determine the association between ONOO$^-$ and POAG and clarify the possibility of RN-NA as a potential tool for POAG diagnosis. Furthermore, the therapeutic value of anti-nitration compounds in IOP management would also be investigated in a nitrative stress mouse model.

SUBJECTS AND METHODS

Ethical Approval Informed consent was obtained for experimentation with human subjects. Moreover, this study was approved by EYE & ENT Hospital, Fudan University of Ethics Committee (KJ2011-04). All procedures in this research were conducted in accordance to the Declaration of Helsinki. Animals were used in accordance with the Association for Research in Vision and Ophthalmology (ARVO) Statement for the Use of Animals in Ophthalmic and Vision Research. All animal experimental protocols were approved by Eye & ENT Hospital, Fudan University (KJ2011-04).

Study Participants Recruited individuals diagnosed with POAG or age-related cataracts (ARC) as the only ocular condition came from the Department of Ophthalmology & Visual Science, Eye & ENT Hospital, Fudan University. POAG was diagnosed by experts in ophthalmology. The inclusion criteria[10] for POAG patients were shown as follows: 1) IOP>21 mm Hg; 2) glaucomatous optic disc damage with corresponding glaucomatous visual field defects; 3) open anterior chamber angle. Patients with previous intraocular surgery, isolated ocular hypertension, other types of glaucoma, other ocular diseases, and systemic diseases were excluded from our study. Ancillary tests were performed on all recruited POAG patients, including visual field testing (Octopus 900 field analyzer) and fundus photography. The axial length (AL), central corneal thickness (CCT), and anterior chamber depth (ACD) were measured by A-mode ultrasound. The IOP was measured by a noncontact tonometer. The refraction and vertical cup-to-disc ratios (VCDR) for all recruited patients were recorded. The ocular parameters from the right eye were applied when patients suffered from POAG or ARC in both eyes.

Sample Collection Plasma and aqueous humor (AH) were extracted from the recruited patients. For surgery preparation, proparacaine hydrochloride was used. AH was obtained at the beginning of the surgical treatment for POAG or ARC by an experienced surgeon through corneal paracentesis *via* a fine-bored needle. The obtained AH samples were immediately transferred to sterilized cryotubes and quickly stored at −80°C. Blood samples were collected from the patients on the day before surgery. The collected blood samples were immediately placed on ice, transported to the laboratory, and then immediately processed by centrifugation at 3000 g at 4°C for 10min. Afterwards, the supernatant was quickly collected and frozen at −80°C.

Synthesis and Characterization of RN-NA The fluorescent probe RN-NA was synthesized and characterized according to our previous work[9]. Briefly, compound RN (0.12 g, 0.24 mmol) and compound NA (0.11 g, 0.25 mmol) were dissolved in 20 mL dimethyl sulfoxide (DMSO) and supplemented with 8.0 mg sodium ascorbate. The mixture was stirred and then reacted at 35°C for 24h after adding to 2 mL of copper sulfate aqueous solution (1 mg/mL). The reaction mixture was detected *via* thin-layer chromatography (TLC), and the crude product was purified *via* column chromatography to obtain compound RN-NA (0.15 g, 0.18 mmol) with 75% yield. The product was stored at 2°C-8°C in a refrigerator until use. The nuclear magnetic resonance (NMR) data were listed as follows: ^{1}H NMR (400 MHz, MeOD-d$_3$) δ 8.30 (s, 2H), 7.99 (s, 2H), 7.75-7.65 (m, 1H), 7.52 (d, *J*=6.5 Hz, 1H), 7.34 (d, *J*=7.2 Hz, 4H), 7.21 (d, *J*=14.1 Hz, 2H), 6.93 (d, *J*=9.3 Hz, 1H), 6.69 (s, 1H),

6.31 (s, 1H), 6.21 (d, J=14.2 Hz, 2H), 4.14 (d, J=7.2 Hz, 4H), 3.57 (d, J=7.0 Hz, 4H), 3.34 (m, 4H), 2.84 (s, 4H), 2.71 (m, 2H), 2.16 (m, 2H), 1.84-1.44 (m, 4H), 1.18-0.73 (m, 6H). 13C NMR (101 MHz, CDCl$_3$) δ 170.06, 167.37, 164.48, 163.78, 156.16, 152.53, 152.19, 149.67, 149.40, 145.00, 137.68, 137.22, 135.56, 134.88, 134.49, 131.76, 131.50, 131.48, 130.59, 130.56, 129.95, 129.26, 128.52, 128.33, 128.14, 127.63, 126.34, 124.96, 124.83, 123.79, 123.47, 122.93, 121.35, 120.46, 120.23, 110.04, 108.84, S3 104.54, 97.31, 66.93, 55.92, 53.07, 44.52, 41.05, 38.93, 35.02, 29.67, 29.26, 27.16, 23.09, 22.30, 12.51. HRMS (ESI) m/z calcd. $C_{52}H_{50}N_7O_6$ [M]$^+$: 868.3817. Found: 868.3798.

The probe RN-NA was prepared from a rhodamine derivative dye (RN, labeled with an azide group) and a naphthalimide derivative dye (NA, labeled with an alkyne group) by a click reaction with 75% yield in State Key Laboratory of Biobased Material and Green Papermaking, Key Laboratory of Pulp & Paper Science and Technology of Shandong Province/Ministry of Education, Qilu University of Technology (Figure 1). The crude product was purified by column chromatography. In the probe, RN was a dye with a red light emission band centered at 650-750 nm, which was sensitive to ONOO$^-$. NA was a relatively stable dye in dilute ONOO$^-$ solution with green light emission at 500-550 nm. The two dyes were used to construct an FRET system with effective energy transfer. When interacting with ONOO$^-$, the red dye was damaged, the red light was turned off, and the green light was enhanced due to the destruction of the FRET process. Therefore, the two dyes in RN-NA were capable of detecting ONOO$^-$ with light changes in the green and red channels.

Measurement of Peroxynitrite The fluorescent probe RN-NA was used to detect ONOO$^-$ directly in Department of Ophthalmology & Visual Science, Eye & ENT Hospital, Fudan University. RN-NA stock solution in 1.0 mmol/L concentration was prepared in DMSO. In ONOO$^-$ fluorescence titration experiments, aliquots of RN-NA was added into phosphate buffered saline (PBS; pH 7.2, 10 mmol/L) first. Then, increasing concentrations of ONOO$^-$ donor 3-morpholinosyndnomine (SIN-1, in 10% NaOH solution) was supplemented in sequence. Subsequently, the mixture were shaken under 37℃, and 10min later, fluorescence spectra were collected on F7100 instrument (Hitachi instrument). After that, the AH (10 µL) or plasma (50 µL) was diluted to 200 µL with PBS then incubated with 20 µmol/L RN-NA at 37℃ for 30min. Next, a microplate reader (Thermo Scientific, USA) was employed for the detection of fluorescence. Notably, the green channel of 540 nm fluorescence was collected with excitation at 488 nm; and the red channel of 710 nm fluorescence was collected with excitation at 633 nm.

Animals Seven female C57BL/6 mice aged 6-8wk were housed in clean cages with loose air filters, a 12-12 hour light-dark cycle, and a temperature of 24℃. The left eye of mice was enrolled in the experimental group (n=7) and the contralateral eye was involved in the control group (n=7). The AH from the mice was collected within 3min of death.

Topical Drug Application SIN-1 solution (ONOO$^-$ donor, 100 µmol/L, 1 µL every drop, Sigma-Aldrich, Shanghai, China) was topically given to the mouse eyes at 8 *a.m.*, 1 *p.m.* and 6 *p.m.* every day for 10 consecutive days. From the 7th day, the mouse eyes were given MnTMPyP (ONOO$^-$ scavenger, 20 mg/mL) with one drop 30min after the SIN-1 application. All eye drops were administered to the central cornea. The vehicle PBS was used as controls in the contralateral eyes.

Intraocular Pressure Measurements in Mice The IOP measurement in both eyes was performed 30min after the last drug treatment using rebound tonometry (TonoLab; ICare, Espoo, Finland) without anesthesia at the same time of day. Every eye was measured three times, and the average was taken as the final measurement.

Statistical Analysis All data were analyzed with SPSS version 27 (SPSS Inc., Chicago, Illinois, USA). The differences of results were compared using independent Student's t-tests or the Mann-Whitney U test. Data were presented as the mean±standard deviation (SD). Receiver operating characteristic (ROC) analysis was adopted to evaluate the ability of ONOO$^-$ to distinguish POAG patients from control subjects. The relationship between ONOO$^-$ level and POAG was analyzed using binary logistic regression. To keep odds ratio (OR) value within reasonable ranges, 10^{-3} was used as unit of ONOO$^-$ level here. Pearson correlation analysis were applied to characterize the relationships between the levels of ONOO$^-$ and the patients' baseline characteristics. In all cases, $P<0.05$ indicated a significant difference.

RESULTS

A total of 200 patients were recruited with 100 POAG patients and 100 ARC patients. Among the 100 POAG patients, 20 cases were in early stage, 47 cases were in medium stage and 33 cases were in advanced stage. Plasma were collected from all the participants, but AH was only collected from 35 POAG patients and 30 ARC patients. The demographic features and ocular parameters of the POAG and ARC patients were shown in Table 1. There was no significant difference in age, gender, refraction, and AL between the POAG and ARC groups, while the IOP and VCDR of the POAG group were significantly higher than those of the ARC group ($P<0.01$).

Synthesis and Spectroscopic Characteristics of RN-NA The spectral behaviors of RN-NA in the presence of ONOO$^-$ were verified to investigate the photophysical properties of the probe. To be specific, a large spectrum response was observed

Table 1 Baseline characteristics of POAG and ARC patients mean±SD

Demographic parameters	AH			Plasma		
	POAG (*n*=35)	ARC (*n*=30)	*P*	POAG (*n*=100)	ARC (*n*=100)	*P*
Age (y)	61.31±11.45	66.67±11.24	0.062	59.70±6.87	61.15±4.60	0.081
Male/female	19/16	13/17	0.459	54/46	48/52	0.479
IOP (mm Hg)	24.95±10.22	14.14±2.83	<0.01	24.86±9.37	14.23±2.68	<0.01
VCDR	0.83±0.10	0.33±0.05	<0.01	0.82±0.10	0.34±0.05	<0.01
AL (mm)	25.15±2.05	24.58±1.59	0.221	24.42±1.57	24.62±1.72	0.392
Refraction (D)	-2.07±2.96	-1.13±2.50	0.176	-1.09±2.80	-1.02±2.87	0.867
MD (dB)	18.07±6.07			16.67±7.60		
CCT (μm)	530±33			536±36		
ACD (mm)	2.79±0.41			2.74±0.47		
POAG stage, *n* (%)						
Early	5 (14.29)			20 (20)		
Medium	17 (48.57)			47 (47)		
Advanced	13 (37.14)			33 (33)		

POAG: Primary open angle glaucoma; ARC: Age-related cataract; AH: Aqueous humor; IOP: Intraocular pressure; VCDR: Vertical cup-to-disc ratios; AL: Axial length; MD: Mean deviation of visual field testing; CCT: Central corneal thickness; ACD: Anterior chamber depth.

in the emission spectra (Figure 2A-2C). With increasing SIN-1 concentration, the fluorescence emission intensity at 550 nm gradually increased, while the fluorescence intensity at 680 nm gradually decreased. When the concentration of SIN-1 reached 50 μmol/L, the fluorescence was almost completely quenched. As shown by the selectivity experiment (Figure 2D), a sharp fluorescence was observed only when ONOO⁻ was presented in the solution. Thus, RN-NA exhibited excellent selectivity toward normal species in biological environment, such as reactive thiols species (Cys, Hcy, and H_2S) and reactive oxygen species (H_2O_2, ClO⁻, and •OH). Such result was consistent with our prediction. Consequently, RN-NA showed high sensitivity to ONOO⁻ and the potential to be a reliable method for detecting ONOO⁻.

Peroxynitrite Levels in the Samples of Patients with Primary Open Angle Glaucoma In the AH, ONOO⁻ levels were significantly higher by 1.07-fold in POAG groups comparing with ARC groups (*P*<0.01; Figure 3A). In the plasma, ONOO⁻ levels were also significantly higher by 1.06-fold in POAG groups comparing with ARC groups (*P*<0.001; Figure 3B).

Association Between Peroxynitrite and Primary Open Angle Glaucoma The ONOO⁻ levels were significantly correlated with POAG in a binary logistic regression analysis. Also, elevated AH and plasma ONOO⁻ level increased the risk of developing POAG [OR=1.008, 95% confidence interval (CI): 1.002-1.013, *P*<0.01 for AH ONOO⁻, OR=1.004, 95%CI: 1.002-1.006, *P*<0.001 for plasma ONOO⁻; Figure 4A]. Furthermore, ROC analysis revealed that the levels of ONOO⁻ in AH and plasma differentiated between POAG patients and control subjects with areas under the curve (AUCs) of 0.6971±0.06806 (95%CI: 0.5638 to 0.8305, *P*<0.05; Figure

4B) and 0.6255±0.03936 (95%CI: 0.5484 to 0.7026, *P*<0.05; Figure 4C), respectively.

Correlations of Peroxynitrite with Clinical Characteristics Linear regression was used to characterize the association of the levels of ONOO⁻ with the patients' age, IOP, and MD of visual field test. The outcomes of Pearson correlation analysis for the level of ONOO⁻ and clinical characteristics revealed that there was no association between the levels of ONOO⁻ and age or IOP (Figure 5A-5D), while the levels of ONOO⁻ in AH or plasma were positively correlated with visual field defects (Figure 5E-5F); the correlation coefficients were 0.51 (*P*<0.01) and 0.45 (*P*<0.001), respectively. Besides, the levels of ONOO⁻ in plasma and AH were correlated in the POAG group (*R*=0.69, *P*<0.001) while not correlated in plasma and AH in the ARC group (Figure 5G-5H).

MnTMPyP Lowers IOP in Ocular Hypertensive Mice Finally, an ocular hypertensive mouse model based on nitrative stress was constructed to investigate the therapeutic value of anti-nitration compounds in IOP management. After treatment with SIN-1 for 4-7d, the treated eyes showed significantly higher IOP and ONOO⁻ levels in the AH compared with the control eyes (*P*<0.05), which indicated that nitrative stress models were successful. By scavenging ONOO⁻ with MnTMPyP, the levels of IOP and ONOO⁻ in AH were significantly lowered after 1, 2, and 3d (Figure 6A-6B). Collectively, scavenging ONOO⁻ in the anterior segment could be a potential way to treat ocular hypertension.

DISCUSSION

In our study, ONOO⁻ in human AH and plasma samples was successfully detected by the highly sensitive fluorescent probe RN-NA. As a result, ONOO⁻ levels were significantly
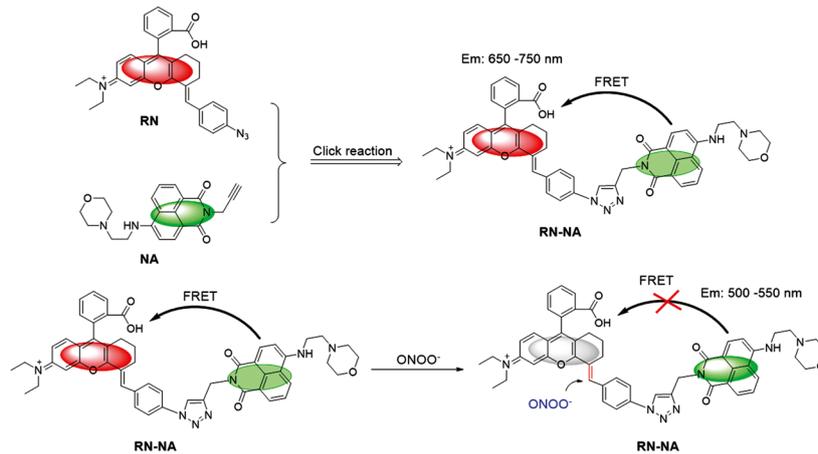
Figure 1 The construction and detection mechanism of RN-NA toward peroxynitrite (ONOO⁻).
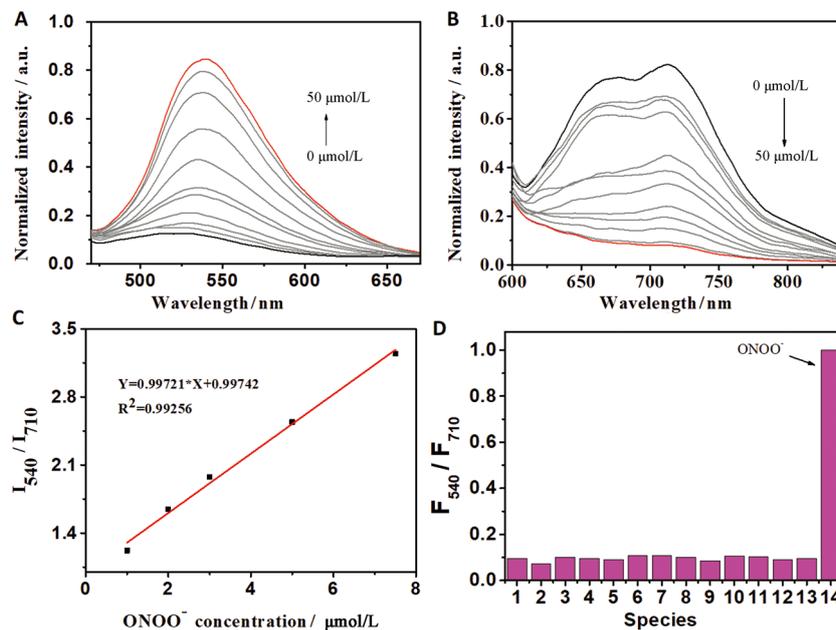

Figure 2 Fluorescence spectrum changes of RN-NA in buffer under SIN-1 titration A, B: Fluorescence spectra changes of 10 μmol/L RN-NA stimulated by SIN-1 at different concentrations in PBS solution (pH=7.4, with 5% DMSO). A: λex=420 nm; B: λex=580 nm; C: Linear fit analysis of fluorescence at ratiometric channel I_{540}/I_{710}; D: Selectivity of RN-NA toward various species, number 1-14 represent Glu, Cys, $S_2O_3^{2-}$, ClO⁻, S^{2-}, SO_3^{2-}, HSO_3^-, NO_2^-, H_2O_2, ·OH, Vc⁻, Zn^{2+}, Fe^{3+}, and ONOO⁻, respectively. Error bar, n=3. SIN-1: 3-morpholinosyndnomine; PBS: Phosphate buffered saline; DMSO: Dimethyl sulfoxide.
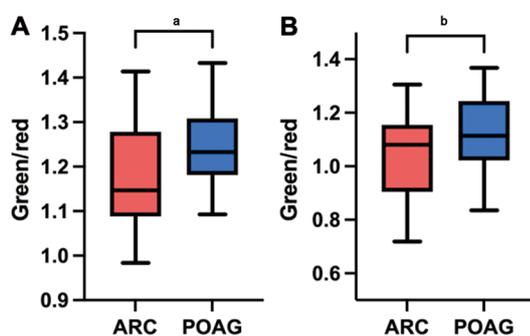

Figure 3 ONOO⁻ levels in the samples of POAG patients ONOO⁻ levels in AH (A) and plasma (B) are significantly higher in POAG groups compared with ARC groups. The data is presented by the box-whiskers plot. A: ARC, n=30, POAG, n=35. B: ARC, n=100, POAG, n=100. [a]$P<0.01$, [b]$P<0.001$. ONOO⁻: Peroxynitrite; POAG: Primary open angle glaucoma; AH: Aqueous humor; ARC: Age-related cataract.

elevated in the plasma and AH of POAG patients compared with control subjects. Additionally, a binary logistic regression analysis disclosed a close correlation between the ONOO⁻ levels and POAG (OR=1.008 for AH ONOO⁻; OR=1.004 for plasma ONOO⁻). Also, ROC analysis suggested that the levels of ONOO⁻ in human plasma and AH could differentiate in group level between POAG patients and control subjects with AUCs of 0.6255±0.03936 and 0.6971±0.06806, respectively. Moreover, a positive correlation was observed between the levels of ONOO⁻ in AH and visual field defects. In an ocular hypertensive mouse model, administering MnTMPyP lowered IOP by scavenging ONOO⁻ in the anterior segment. Thus, we conclude that ONOO⁻ is a novel biomarker and a potential treatment target of POAG especially advanced POAG for ocular hypertension.
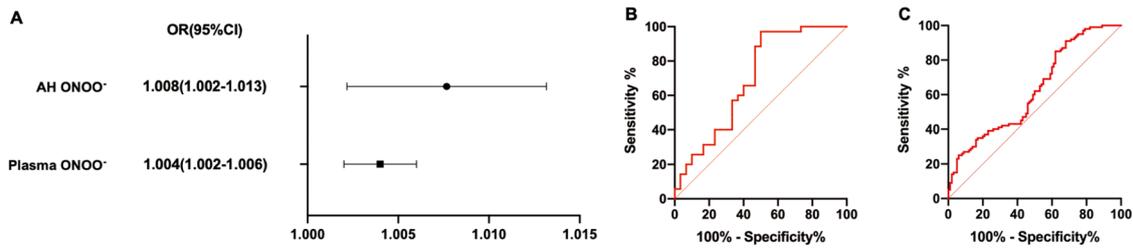
Figure 4 Association of ONOO⁻ with POAG A: Forest plot of POAG risk associated with ONOO⁻ levels. Horizontal lines indicate 95%CI. Elevated AH and plasma ONOO⁻ level increases the risk of developing POAG (OR=1.008, 95%CI: 1.002-1.013, *P*<0.01 for AH ONOO⁻, OR=1.004, 95%CI: 1.002-1.006, *P*<0.001 for plasma ONOO⁻). B-C: Power of AH (B) and plasma (C) of ONOO⁻ in differentiating POAG patients from ARC patients. The respective AUC are 0.6971±0.06806 (95%CI: 0.5638 to 0.8305) and 0.6255±0.03936 (95%CI: 0.5484 to 0.7026). OR: Odds radio; CI: Confidence interval; POAG: Primary open angle glaucoma; AH: Aqueous humor; ONOO⁻: Peroxynitrite; ARC: Age-related cataract; AUC: Areas under the curve.
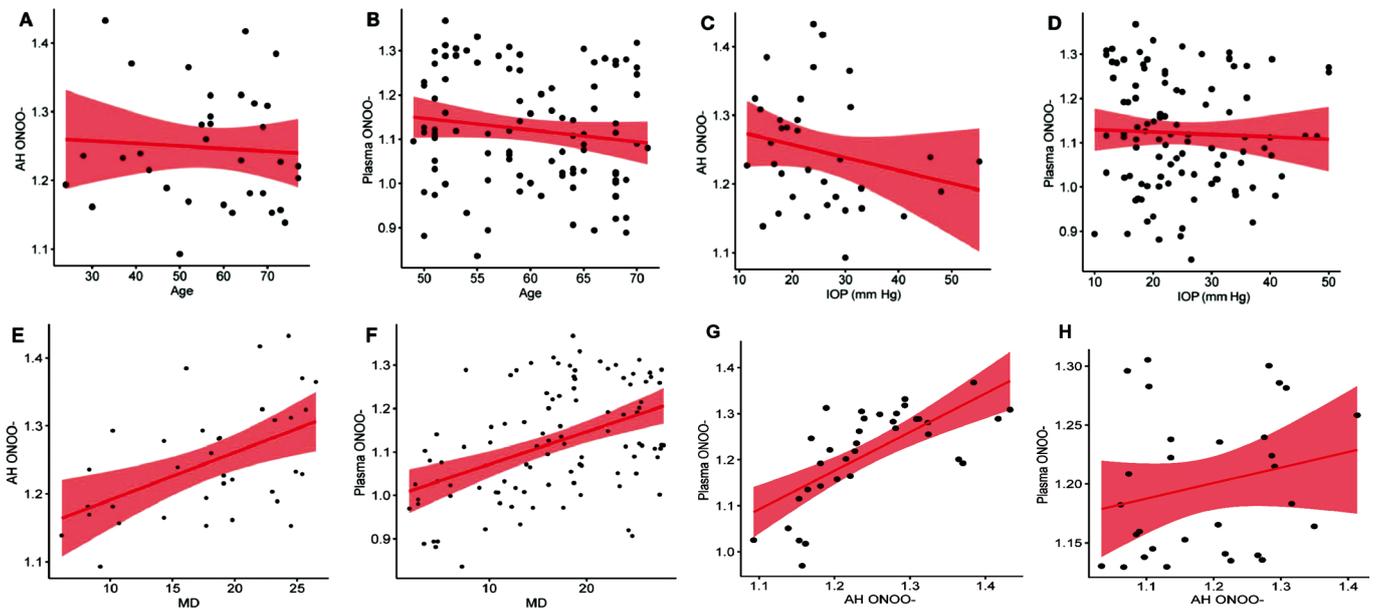

Figure 5 The association of ONOO⁻ and age, IOP or visual field defects A, B: Linear regression was used to characterize the relationship of the levels of ONOO⁻ with the patients' age in AH (A; *n*=35, *R*=-0.066, *P*=0.71) or plasma (B; *n*=100, *R*=-0.14, *P*=0.15). C, D: Linear regression was used to characterize the relationship of the levels of ONOO⁻ with the patients' IOP in AH (C; *n*=35, *R*=-0.23, *P*=0.19) or plasma (D; *n*=100, *R*=-0.039, *P*=0.7). E, F: Positive correlation was found between visual field defects and the levels of ONOO⁻ in AH (E, *n*=35, *R*=0.51, *P*=0.002) or plasma (F, *n*=100, *R*=0.45, *P*<0.001). G, H: The levels of ONOO⁻ in plasma and AH were correlated in the POAG group (G; *n*=35, *R*=0.69, *P*<0.001) while no correlation between the levels of ONOO⁻ in plasma and AH were observed in the ARC group (H; *n*=30, *R*=0.23, *P*=0.23). *R* stands for correlation coefficient. ONOO⁻: Peroxynitrite; AH: Aqueous humor; IOP: Intraocular pressure; POAG: Primary open angle glaucoma; ARC: Age-related cataract.
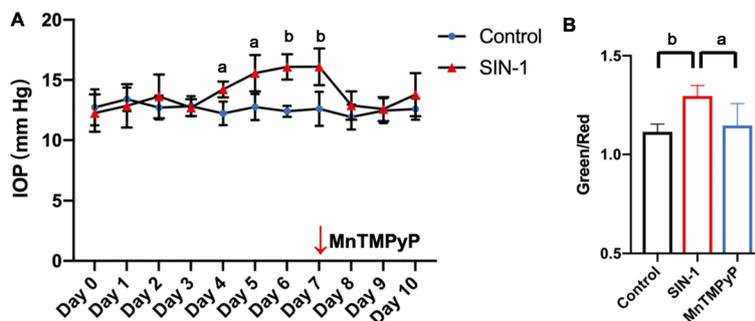

Figure 6 SIN-1 elevates IOP by externally supplying ONOO⁻ and MnTMPyP significantly reduces IOP by scavenging ONOO⁻ A: Changes in IOP after administering SIN-1 and MnTMPyP to the central cornea (*n*=7). PBS was used as controls in the contralateral eyes (*n*=7). After treatment with SIN-1 for 4-7d, the treated eyes showed significantly higher IOP. B: AH ONOO⁻ levels tested by RN-NA after administering SIN-1 and MnTMPyP. By scavenging ONOO⁻ with MnTMPyP, the levels of IOP and AH ONOO⁻ were significantly lowered. ᵃ*P*<0.05, ᵇ*P*<0.01. IOP: Intraocular pressure; SIN-1: 3-Morpholinosyndnomine; ONOO⁻: Peroxynitrite; PBS: Phosphate buffered saline; AH: Aqueous humor.

Owing to low abundance and short half-life, the detection of ONOO⁻ is challenging[11]. 3-NT is the main chemical product of nitrative stress, so it has been widely used as a diagnostic footprint. Currently, enzyme-linked immunosorbent assay (ELISA) and Western blot (WB) analysis based on specific 3-NT antibodies are the most commonly used methods to detect ONOO⁻. However, cross-reactivity and/or epitope preference may occur when using anti-nitration antibodies for ELISA or WB. More importantly, 3-NT cannot directly represent the total amount of ONOO⁻ because tyrosine nitration is a low-yield process, and a relatively small amount of proteins are found to be significantly nitrated in cells and tissues[11]. Other nitrative stress processes, such as DNA damage or lipid nitration, could not be reflected by detecting 3-NT. In comparison, RN-NA was more cost effective and more accurate than the conventional methods for the measurement of ONOO⁻. The detection of ONOO⁻ in clinical settings has been significantly improved due to the development of RN-NA.

Several methods, such as electrochemical methods, electron spin resonance, fluorescence microscopy have been developed for the measurement of ONOO⁻[11]. Among them, fluorescence microscopy has the characteristics of a fast response, high sensitivity, and real-time detection[12-13]. A multifunctional fluorescence platform RN-NA was constructed based on the FRET process for the rapid detection of ONOO⁻. It responds to ONOO⁻ by exhibiting remarkable green/red fluorescence changes[9]. In our study, a fast and stable method was constructed to detect ONOO⁻ levels in plasma and AH. Notably, this method only required a small amount of plasma (50 µL) or AH (10 µL). To be specific, through some simple operations and within a short time (approximately 40min), ONOO⁻ levels could be measured by measuring red/green fluorescence using a microplate reader. such method is suitable for the rapid testing of clinical samples.

ONOO⁻ is involved in a number of physiological processes and diseases, such as neurodegeneration, cardiovascular diseases, and glaucoma. In Parkinson's disease, plasma ONOO⁻ levels are significantly increased[14]. Neurotoxic modifications closely associated with the destruction of key molecules and inactivation of antioxidant enzymes can be mediated by nitrative stress damage. In cardiovascular diseases, some proteins, such as apoA-I, fibronectin, and laminin, are nitrated by ONOO⁻-associated pathways, which can cause endothelial dysfunction[15]. One of the reasons of endothelial dysfunction may be tyrosine nitration. Furthermore, reduced adhesion and cell spreading can be observed in endothelial cells grown on ONOO⁻-modified fibronectin[16].

Our data suggested that ONOO⁻ was a biomarker for POAG with high ROC sensitivity in human AH samples (Figure 4). The increased 3-NT level in the trabecular meshwork cells may decrease the cell population[17]. As shown in Figure 5 in this study, ONOO⁻ in AH was significantly related to the visual field defects in POAG patients. Hence, it is possible that circulating ONOO⁻ in the retina could trigger the onset of retinopathy and cause corresponding visual field defects. In nerve cells, ONOO⁻ inhibits the mitochondrial respiratory chain and causes mitochondrial damage, ultimately leading to nerve cell death[18]. As the extent of visual field defects is often related to the stage of POAG and the advanced POAG patients have severer visual field defects, we speculate that the ONOO⁻ levels in POAG may associated with the disease stage of the POAG. However, the sample size in this study is small and most of the patients have medium stage of POAG, which may cause large bias in subgroup analyses. Therefore, the relationship between ONOO levels and POAG stage needs to be further verified in future studies.

Exposure to ONOO⁻ led to IOP elevation in mouse models[8,19], which could be reversed by antioxidant application (Figure 6). However, there is not enough evidence regarding which specific tyrosine nitrated proteins are involved in the pathogenesis of POAG. Reduced AH outflow and elevated IOP are related to increased Rho/ROCK signaling activity[20-21]. Interestingly, nitration of Tyr34 in RhoA can enhance the response to AngII-induced contraction and modulate Rho/ROCK signaling[22]. Several drugs blocking nitration have already been investigated for the treatment of endothelial dysfunction. HMG-CoA inhibitors (statins) can reduce the ONOO⁻ level and restore the NO/ONOO⁻ imbalance, producing antiatherosclerotic effects[23-24]. A porphyrinic ONOO⁻ decomposition catalyst, FP15, can improve myocardial function after cardiopulmonary bypass[25]. One of the ONOO⁻ scavengers, FeTMPyP, can improve resistance artery performance in aging rats[26]. In a nutshell, it is reasonable that ONOO⁻ scavengers have promising therapeutic potential due to nitrative stress damage affecting endothelial function and AH outflow. MnTMPyP is a metalloporphyrin that contains a porphyrin ring and a Mn center, which acts as an ONOO⁻ decomposition catalyst[27]. Working as a cell permeable substance, MnTMPyP can lessen toxic effects of ONOO⁻. Both previous studies and our studies proved that IOP elevation caused by nitrative stress could be reversed by MnTMPyP application[19,28]. Overall, it is a promising ONOO⁻ scavenger for treating elevated IOP by protecting AH outflow from nitrative stress damage.

In conclusion, ONOO⁻ levels in AH and plasma are significantly correlated with POAG and positively correlated with visual field defects in POAG patients, which suggests that ONOO⁻ is a potential biomarker of POAG especially advanced POAG. Besides, IOP elevation caused by nitrative stress can be

reversed by MnTMPyP application. This study has paved the way for RN-NA serving as a potential clinical tool in a variety of nitrative stress related-diseases and revealed the therapeutic value of anti-nitration compounds in IOP management.

REFERENCES

1 Jonas JB, Aung T, Bourne RR, Bron AM, Ritch R, Panda-Jonas S. Glaucoma. *Lancet* 2017;390(10108):2183-2193.

2 Stein JD, Khawaja AP, Weizer JS. Glaucoma in adults-screening, diagnosis, and management: a review. *JAMA* 2021;325(2):164-174.

3 Wu X, Wang Y, Liu X, Li ZH, Deng LQ, Chen DS, Wang DJ. Outcomes of chronic angle-closure glaucoma treated by phacoemulsification and endocyclophotocoagulation with or without endoscopically goniosynechialysis. *Int J Ophthalmol* 2022;15(8):1273-1278.

4 Aslan M, Cort A, Yucel I. Oxidative and nitrative stress markers in glaucoma. *Free Radic Biol Med* 2008;45(4):367-376.

5 Andrabi SM, Sharma NS, Karan A, Shatil Shahriar SM, Cordon B, Ma B, Xie JW. Nitric oxide: physiological functions, delivery, and biomedical applications. *Adv Sci* 2023;10(30):e2303259.

6 Bandookwala M, Thakkar D, Sengupta P. Advancements in the analytical quantification of nitroxidative stress biomarker 3-nitrotyrosine in biological matrices. *Crit Rev Anal Chem* 2020;50(3):265-289.

7 Ferrer-Sueta G, Campolo N, Trujillo M, Bartesaghi S, Carballal S, Romero N, Alvarez B, Radi R. Biochemistry of peroxynitrite and protein tyrosine nitration. *Chem Rev* 2018;118(3):1338-1408.

8 Lei Y, Gao YT, Song MM, Cao WJ, Sun XH. Peroxynitrite is a novel risk factor and treatment target of glaucoma. *Nitric Oxide* 2020;99:17-24.

9 Bao L, Liu KY, Chen YL, Yang GH. Construction of a rational-designed multifunctional platform based on a fluorescence resonance energy transfer process for simultaneous detection of pH and endogenous peroxynitrite. *Anal Chem* 2021;93(26):9064-9073.

10 Weinreb RN, Khaw PT. Primary open-angle glaucoma. *Lancet* 2004;363(9422):1711-1720.

11 Möller MN, Rios N, Trujillo M, Radi R, Denicola A, Alvarez B. Detection and quantification of nitric oxide-derived oxidants in biological systems. *J Biol Chem* 2019;294(40):14776-14802.

12 Wang Z, Zhang F, Xiong JH, Mao ZQ, Liu ZH. Investigations of drug-induced liver injury by a peroxynitrite activatable two-photon fluorescence probe. *Spectrochim Acta A Mol Biomol Spectrosc* 2021;246:118960.

13 Liu JJ, Dong YY, Ma YX, Han YX, Ma SD, Chen HL, Chen XG. One-step synthesis of red/green dual-emissive carbon dots for ratiometric sensitive ONOO⁻ probing and cell imaging. *Nanoscale* 2018;10(28):13589-13598.

14 Kouti L, Noroozian M, Akhondzadeh S, Abdollahi M, Javadi MR, Faramarzi MA, Mousavi S, Ghaeli P. Nitric oxide and peroxynitrite serum levels in Parkinson's disease: correlation of oxidative stress and the severity of the disease. *Eur Rev Med Pharmacol Sci* 2013;17(7):964-970.

15 Peluffo G, Radi R. Biochemistry of protein tyrosine nitration in cardiovascular pathology. *Cardiovasc Res* 2007;75(2):291-302.

16 Jiang M, Zhao XM, Jiang ZS, Wang GX, Zhang DW. Protein tyrosine nitration in atherosclerotic endothelial dysfunction. *Clin Chim Acta* 2022;529:34-41.

17 Fernández-Durango R, Fernández-Martínez A, García-Feijoo J, Castillo A, de la Casa JM, García-Bueno B, Pérez-Nievas BG, Fernández-Cruz A, Leza JC. Expression of nitrotyrosine and oxidative consequences in the trabecular meshwork of patients with primary open-angle glaucoma. *Invest Ophthalmol Vis Sci* 2008;49(6):2506-2511.

18 Zhang YF, He YC, Wu ML, Chen HS, Zhang L, Yang D, Wang Q, Shen JG. Rehmapicroside ameliorates cerebral ischemia-reperfusion injury via attenuating peroxynitrite-mediated mitophagy activation. *Free Radic Biol Med* 2020;160:526-539.

19 Hu CC, Zhang Y, Song MM, Deng YH, Sun XH, Lei Y. Prolonged use of nitric oxide donor sodium nitroprusside induces ocular hypertension in mice. *Exp Eye Res* 2021;202:108280.

20 Clement Freiberg J, von Spreckelsen A, Kolko M, Azuara-Blanco A, Virgili G. Rho kinase inhibitor for primary open-angle glaucoma and ocular hypertension. *Cochrane Database Syst Rev* 2022;6(6):CD013817.

21 Honjo M, Tanihara H. Impact of the clinical use of ROCK inhibitor on the pathogenesis and treatment of glaucoma. *Jpn J Ophthalmol* 2018;62(2):109-126.

22 Rafikov R, Dimitropoulou C, Aggarwal S, Kangath A, Gross C, Pardo D, Sharma S, Jezierska-Drutel A, Patel V, Snead C, Lucas R, Verin A, Fulton D, Catravas JD, Black SM. Lipopolysaccharide-induced lung injury involves the nitration-mediated activation of RhoA. *J Biol Chem* 2014;289(8):4710-4722.

23 Heeba G, Moselhy ME, Hassan M, Khalifa M, Gryglewski R, Malinski T. Anti-atherogenic effect of statins: role of nitric oxide, peroxynitrite and haem oxygenase-1. *Br J Pharmacol* 2009;156(8): 1256-1266.

24 Almeida SO, Budoff M. Effect of statins on atherosclerotic plaque. *Trends Cardiovasc Med* 2019;29(8):451-455.

25 Radovits T, Beller CJ, Groves JT, Merkely B, Karck M, Szabó C, Szabó G. Effects of FP15, a peroxynitrite decomposition catalyst on cardiac and pulmonary function after cardiopulmonary bypass. *Eur J Cardiothorac Surg* 2012;41(2):391-396.

26 Sun Q, Dong Y, Wang HY, Jiao K, Xu JH, Ma L, Huang HX, Liu HR, Wang W. Antiperoxynitrite treatment ameliorates vasorelaxation of resistance arteries in aging rats: involvement with protection of circulating endothelial progenitor cells. *J Cardiovasc Pharmacol* 2016;68(5):334-341.

27 Li JY, Wei JJ, Gao ZH, Yin GC, Li HL. The oxidative reactivity of three manganese(III) porphyrin complexes with hydrogen peroxide and nitrite toward catalytic nitration of protein tyrosine. *Metallomics* 2021;13(3):mfab005.

28 Li LP, Zhou J, Fan WP, Niu LL, Song MM, Qin B, Sun XH, Lei Y. Lifetime exposure of ambient $PM_{2.5}$ elevates intraocular pressure in young mice. *Ecotoxicol Environ Saf* 2021;228:112963.